

Measurements of turbulent particle fluxes in the dry CBL over a continental European site with combined wind lidar and multiwavelength Raman lidar

Ronny Engelmann¹, Albert Ansmann¹, Ulla Wandinger¹, Dietrich Althausen¹, and Detlef Müller^{1,2}

¹Leibniz Institute for Tropospheric Research (IfT), Permoserstr. 15, 04318 Leipzig, Germany
Correspondence to: R. Engelmann (ronny@tropos.de)

²Atmospheric Remote Sensing Laboratory, Gwangju Institute of Science and Technology, Republic of Korea

1. INTRODUCTION

The turbulent transport of aerosol particles between the planet's surface and the lower troposphere has a strong influence on atmospheric composition, long-range aerosol transport, and cloud formation as well as on smog and haze conditions at the ground. Vertical exchange depends in a complicated way on surface characteristics and meteorological conditions in the planetary boundary layer (PBL). The mechanisms of turbulent transport within the PBL and in the entrainment zone, the region between the PBL and the free troposphere, are not well understood and thus are not well parameterized in atmospheric models. Therefore, respective observations are of high interest. With the IfT lidar instrumentation the vertical wind as well as aerosol properties can be determined with high spatial and temporal resolution.

Our aim is to quantify the vertical particle exchange throughout the PBL. The respective turbulent mass fluxes were obtained from unique simultaneous measurements with a Doppler wind lidar and an aerosol Raman lidar. The observations were performed in the outer region of Leipzig at the IfT in 2006/07 and cover meteorological situations in which the majority of the turbulent flux was caused by large eddies in the convective boundary layer (CBL).

2. EXPERIMENT

The portable wind lidar [2] was set up close to the laboratory three-wavelength Raman lidar of IfT [4] with a horizontal distance of <10 m. Both systems were synchronized on a fixed time grid every 5 s.

The institute is located in the eastern suburbs of Leipzig. The city is surrounded by flat terrain. The Raman lidar and the wind lidar were used to measure coherent datasets of aerosol backscatter and corresponding vertical wind speed during daytime. The measurement with the Raman lidar was extended until nighttime to obtain accurate data for a characterization of microphysical aerosol properties. Figure 1 presents the PBL development during daytime between 1000 and 1100 UTC (1200 and 1300 local time, Central European Time) and between 1200-1300 UTC on 26 April 2007. The particle backscatter coefficient at 532 nm and the vertical wind speed are displayed and show very good correlations for the first time interval. Thermal updraft regions with increased backscatter (yellow and red on

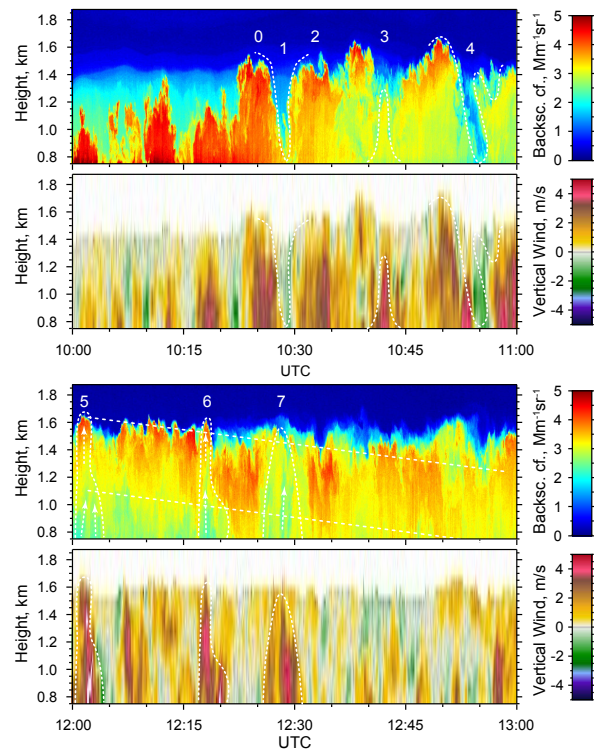


Figure 1: Temporal development of the CBL at Leipzig on 26 April 2007. The top panels show the particle backscatter coefficient at 532 nm, the lower panels show the vertical wind speed.

the plot of the vertical wind, see markers 0,2,3) can be clearly distinguished from downward mixing processes of clean air (green, see markers 1,4). This positive correlation clearly indicates a turbulent upward transport of aerosol particles. In contrast, later during the day and especially at a lower height a decreased backscatter coefficient is often found in the thermal updrafts (see 5, 6, 7). For these cases cleaner air is mixed upwards while more polluted air is transported downwards. This anti-correlation of vertical wind speed and backscatter coefficient indicates a negative turbulent aerosol flux.

3. DATA EVALUATION SCHEME

The method which is shown in Fig. 2 was developed in order to determine vertical profiles of turbulent particle mass fluxes exclusively from lidar observations (based

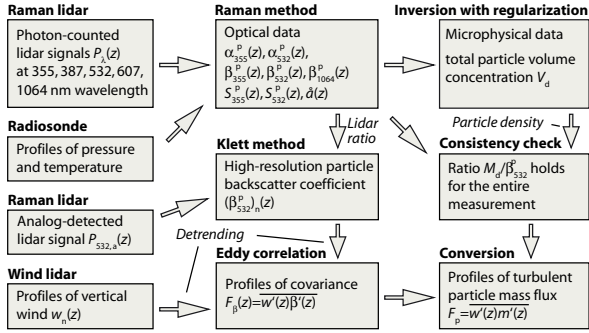


Figure 2: Data evaluation scheme for the calculation of the turbulent aerosol mass flux.

on [2]). For ground-based profile observations Taylor's frozen turbulence hypothesis must be applied, i.e., it is assumed that the temporally resolved datasets well represent the spatial average. Then the eddy-correlation technique can be used and the turbulent flux F_p of the particle mass concentration $m = M_d + m'$ is given by the covariance between m and the vertical wind speed w : $F_p = \langle m'w' \rangle$. The prime indicates deviations from the mean value and the brackets represent the temporal average. By definition, updrafts have a positive sign, and positive values of F_p imply upward fluxes.

Typically, from lidar observations only the particle backscattering can be determined with sufficient temporal resolution for the application of the eddy-correlation technique. Therefore, the time series of the 532-nm particle backscatter coefficient β_{532}^p with a resolution of 5 s was used for the calculation. Thus the primary output of the flux calculation is the covariance $F_\beta = \langle \beta'w' \rangle$.

In a second step, multiwavelength Raman lidar observations (extinction coefficients α^p at 355 and 532 nm, backscatter coefficients β^p at 355, 532, 1064 nm) were used and microphysical particle parameters could be derived with an inversion scheme [5, 1]. In this way, among other quantities, profiles of the particle volume concentration V_d were obtained with low temporal resolution. The mean particle mass concentration M_d was estimated by assuming a typical particle density.

In the third step, it has to be ensured that the obtained relationship between β_{532}^p and M_d holds for the entire measurement region, so that any change of β_{532}^p with height and any fluctuations β' are caused by respective changes in the mass concentration M_d and its fluctuations m' . Then the turbulent aerosol mass flux at the height z is given by $F_p(z) = M_d/\beta_{532}^p \langle \beta'(z)w'(z) \rangle$. The simplification of a height- and time-independent conversion factor M_d/β_{532}^p implies that the aerosol size distribution and the particle chemical composition do not vary in the CBL during a measurement.

4. RESULTS

From the Raman lidar measurements after sunset we derived the profiles of the optical particle parameters. Figure 3 shows the analysis of this measurement. The values of the lidar ratios S^p of 52 and 53 sr for 355 and 532 nm, respectively, and the Ångström exponent \tilde{a} of 1.5 are typical for anthropogenic aerosol particles in Central Europe and indicate low absorbing particles that mainly stem from agricultural or rural sources.

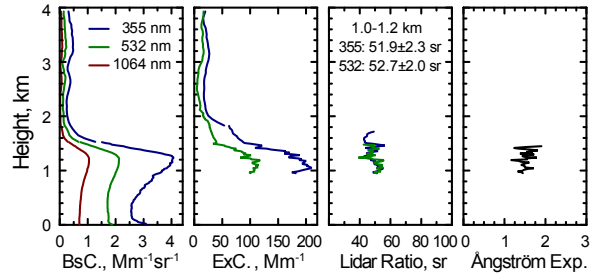


Figure 3: Multiwavelength Raman lidar observation of three backscatter and two extinction coefficients from 1935–2147 UTC on 26 April 2007. Respective profiles of lidar ratios and the Ångström exponent are also given.

The mean values of the three backscatter coefficients and the two extinction coefficients from a height interval at the top of the PBL (1.0–1.2 km) were selected for lidar data inversion. The input data for the inversion as well as the results are summarized in Tab. 1. The results from the inversion are in good agreement with the surface-based observation with a Differential Mobility Particle Spectrometer (DMPS). Particles with a diameter smaller than 160 nm were neglected from the DMPS data for comparison purposes because the inversion is insensitive to such small particles. However, this small particle regime only contains less than 10% of the total volume concentration. The standard deviations from the single DMPS scans within the two time intervals 12–18 and 18–24 UTC are also given in the table.

Table 1: Input data and inversion results for 26 April 2007. The optical data at different wavelengths λ are averaged for the height range from 1.0–1.2 km. The ground-based DMPS measurements were averaged from 12–18 UTC and from 18–24 UTC. The M_d/β_{532}^p factor was derived with a mean particle density of 1.6 g cm^{-3} .

λ , nm	355	532	1064
β , $\text{Mm}^{-1} \text{sr}^{-1}$	3.9	2.1	1.0
α , Mm^{-1}	201	110	
S^p , sr	52	53	
$\tilde{a}_{355-532}$	1.5 ± 0.2		
Microphysical data	Lidar	DMPS 12–18	DMPS 18–24
r_{eff} , nm	180 ± 40	144 ± 13	145 ± 17
V_d , $\mu\text{m}^3 \text{cm}^{-3}$	18 ± 8	20.4 ± 1.8	18.6 ± 2.1
M_d/β_{532}^p , $\mu\text{g m}^{-3} \text{Mm sr} \rightarrow 13.8 \pm 6.1$			

The derived volume concentration of $18 \pm 8 \mu\text{m}^3 \text{cm}^{-3}$ was used for the further treatment of the aerosol mass flux. With a typical particle density of 1.6 g cm^{-3} a backscatter-to-mass conversion factor of $13.8 \pm 6.1 \mu\text{g m}^{-3} \text{Mm sr}$ was derived for 26 April 2007. The mean Ångström exponent \tilde{a} which was derived for the height level 1.0–1.2 km was found to be 1.5 ± 0.2 (see Fig. 3). IfT's AERONET Sun photometer data were available and could be compared to lidar-derived values. Figure 4 shows the time series of the aerosol optical depth for the wavelengths 340, 500, and 1020 nm, which are close to the lidar wavelengths. In the morning

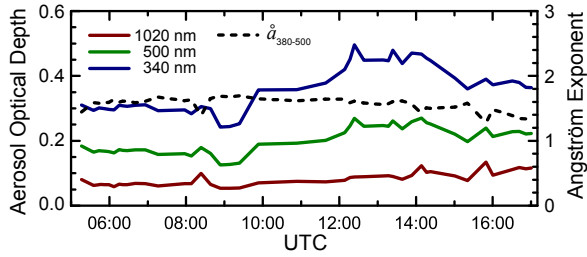


Figure 4: Time series of aerosol optical depth and Ångström exponent measured with IfT's AERONET Sun photometer on 26 April 2007.

hours until 0830 UTC the values remain rather constant at about 0.17 for 500 nm. At around 1100–1200 UTC an increase of about 50% is observed.

The AERONET-derived Ångström exponents between 380–500 nm were found to be 1.4–1.6. These values remain constant during the entire day, especially during the period of increased values of the optical depth. They also compare well with the lidar-derived value from the nighttime measurement. It can be stated from this finding that the aerosol composition in the PBL did not vary significantly during the entire day and that the M_a/β_{532}^p ratio holds for the entire measurement. Therefore, the microphysical particle properties, which were derived from the nighttime measurements, can be used for the conversion of $\overline{w'\beta'}$ to aerosol mass fluxes.

In Fig. 5 the cospectra $C_{w,\beta}$ of the vertical wind and the particle backscatter coefficient, i.e. the spectral decomposition of the turbulent flux, are shown for different time periods during the day and for a height level of 975 m. The top axes has been derived with the occurring wind speed of 5 m s^{-1} . The presentation of the cospectra over the frequency ν is given as $\nu C_{w,\beta}$ vs. $\log \nu$ in order to preserve the area and to give a realistic weight to high frequencies.

From 0930–1100 UTC an upward flux (positive area of the cospectrum) can be observed within a frequency range of 10^{-2} – 10^{-3} Hz. This corresponds to eddy sizes of 400–5000 m. The largest particle flux components stem from horizontal eddy dimensions of 2.1 km, i.e., the dominant eddies are deformed by a factor of 1.5 in the horizontal direction, because the CBL height for this time interval was about 1.4 km.

Later during the day, we see—as already discussed in the context of Fig. 1—that a downward flux is present at the height level of 975 m. The involved eddy sizes are 500–4000 m. The strongest peak for the time interval 1100–1230 UTC is found at 3 km. It remains unclear whether this length corresponds to heavily deformed eddies (factor 2) or to an ordered structure of turbulence and large-scale features in the CBL that are often found in atmospheric flows. In addition, we find that 90-min averaging intervals for the flux calculations are reasonable for the atmospheric situation because the cospectra approach zero values at both ends of the frequency range.

Hence the profiles of the vertical particle fluxes on 26 April 2007 were derived for intervals of 90 min and are shown in Fig. 6. The abscissa axis for the aerosol mass flux was derived from the $\beta'w'$ axis by the factor given in Tab. 1. The maximum heights of the flux profiles were defined by the point at which the number of invalid

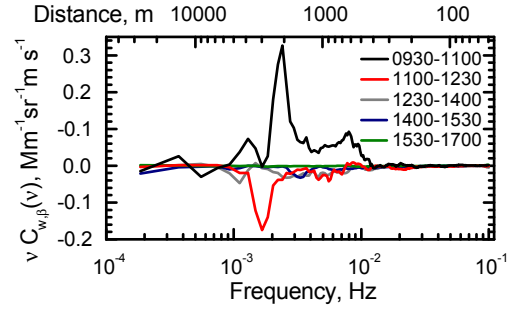


Figure 5: Cospectra of the vertical-wind and backscatter-coefficient fluctuations at a height level of 975 m. The top axes have been converted with a wind speed of 5 m/s.

data points in the wind time series, because of weak signals in clean air, reached 1/3 of the total number of data points. The error bars show the largest uncertainty that is caused by the dominant sampling error during a ground based flux measurement [3].

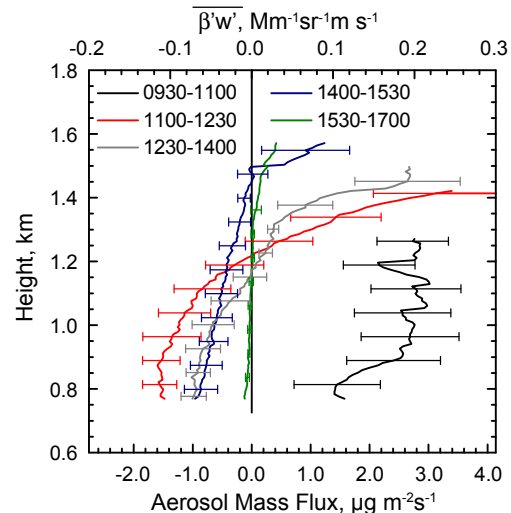


Figure 6: Profiles of the turbulent aerosol mass flux for five time intervals of 90 min each at Leipzig on 26 April 2007. Mean and standard deviations are given.

Between 0930 and 1100 UTC the highest flux values were found at the quickly mixing CBL top. These maximum values of 2.5 – $3.0 \mu\text{g m}^{-2}\text{s}^{-1}$ remained rather constant in the entrainment zone during the most active convection period between 0930 and 1400 UTC. After 1400 UTC the convection slowed down and the vertical exchange processes settled, resulting in nearly zero flux values from 1530–1700 UTC.

It was found that from 1100–1230 and 1230–1400 UTC the sign of the vertical flux changed at a height of about 1200 m. While upward fluxes were still observed at the CBL top (entrainment zone), there was turbulent downward mixing below because of a higher aerosol content that occurred in the upper CBL at that time. This downward flux of about $-(1.5$ – $1.0) \mu\text{g m}^{-2}\text{s}^{-1}$ almost reached half the magnitude of the upward entrainment flux.

From 1400–1530 UTC the entrainment at the top of the PBL decreased. However, the downward mixing was still ongoing. The respective flux profile is not constant with height. Moreover, the downward mixing was more

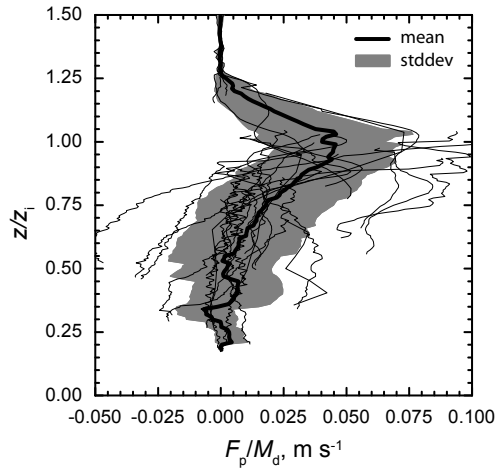


Figure 7: Normalized profiles of all obtained aerosol mass flux profiles during the convective measurement periods. Shown are the single profiles (thin lines), the mean profile, and the standard deviation.

efficient for lower heights. This can be explained by the suppressed convection because of the decreased incoming solar radiation in the afternoon. In this context the vertical extent of the eddy dimensions decreased. Hence the absolute aerosol transport by convective turbulence was greater at lower altitudes in the late afternoon. Between 1530 and 1700 UTC the convection slowed down and therefore turbulent particle fluxes approached values close to zero.

Five further days with dry CBL developments during the measurement period 2006/07 were evaluated and the profiles of the vertical aerosol mass fluxes could be determined. Figure 7 shows these profiles which were normalized for the CBL height and for the mean aerosol mass concentration M_d on these days. For this analysis, M_d was directly derived from the regularly DMPS measurements, assuming a particle density of 1.6 g cm^{-3} . In this scaled representation, entrainment fluxes of $(0.045 \pm 0.025) \text{ m s}^{-1} \times M_d$ were found on average.

Furthermore, the growth rates of the CBL were derived from the lidar measurements and could be compared to the predicted growth rates from the obtained entrainment fluxes. Using the simple assumption of horizontal homogeneity, it can be assumed that the entrainment flux is directly linked to the CBL growth. Figure 8 shows the correlation between the CBL growth rates and the entrainment fluxes divided by the mean aerosol mass concentration in the mixing layer. A correlation coefficient of 0.7 was found. It can be seen that the observed growth rates are significantly lower than the predicted ones. We assume that this fact can be explained by a simultaneous deposition flux at the ground, since the mean aerosol mass concentration observed with DMPS did not significantly increase during the time of the measurement periods.

5. CONCLUSIONS AND OUTLOOK

A method was developed and applied for the characterization of the comprehensive life cycle of atmospheric aerosol particles within the PBL with special emphasis on vertical transport. In the sense of a feasibility study

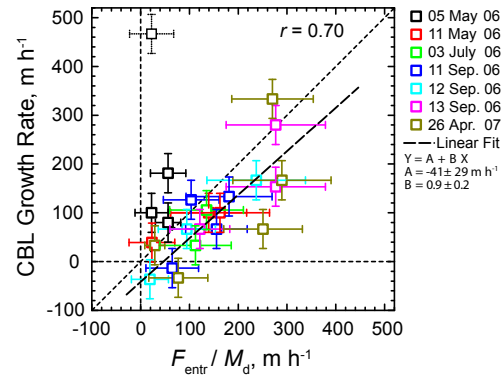


Figure 8: Growth rates versus the entrainment flux F_{entr}/M_d for the cases of dry-boundary-layer observations. The outlier on 5 May (top left) was removed for the linear fit.

the great potential of this method was shown. For the first time it is possible to quantify the vertical aerosol transport throughout the entire PBL, even up to the entrainment zone.

The future work includes special characterization of the vertical exchange processes with respect to humidity growth of aerosol. Many open questions still remain on how non-conservative scalars (like the ambient aerosol mass in humid environments) should be treated. Additionally, the process of vertical transport of aerosol particles into clouds is of high interest.

Therefore experiments with combined measurements of temperature and water-vapor concentrations are necessary. These two parameters play an important role for the alteration of aerosol particles. Nowadays, these data can be determined from lidar measurements with the appropriate systems on the time scale of 30–60 s, which is appropriate for flux measurements in the CBL, too.

REFERENCES

- [1] A. Ansmann and D. Müller. Lidar and atmospheric aerosol particles. In C. Weitkamp, editor, *Lidar: Range-Resolved Optical Remote Sensing of the Atmosphere*, pages 105–141. Springer, New York, USA, 2005.
- [2] R. Engelmann, U. Wandinger, A. Ansmann, D. Müller, E. Žeromskis, D. Althausen, and B. Wehner. Lidar observations of the vertical aerosol flux in the planetary boundary layer. *J. Atmos. Oceanic Technol.*, **25**, 1296–1306, 2008.
- [3] D. Lenschow, J. Mann, and L. Kristensen. How long is long enough when measuring fluxes and other turbulent statistics? *J. Atmos. Oceanic Technol.*, **11**, 661–673, 1994.
- [4] I. Mattis, A. Ansmann, D. Althausen, V. Jaenisch, U. Wandinger, D. Müller, Y. Arshinov, S. Bobrovnikov, and I. Serikov. Relative-humidity profiling in the troposphere with a Raman lidar. *Appl. Opt.*, **41**, 6451–6462, 2002.
- [5] D. Müller, U. Wandinger, D. Althausen, and M. Fiebig. Comprehensive particle characterization from three-wavelength Raman-lidar observations. *Appl. Opt.*, **40**, 4863–4869, 2001.